

Speed distributions of the photofragments of vinyl chloride determined by direct inversion of Doppler profiles

Yibo Huang, Guoxin He, Yungan Yang, Satoshi Hashimoto¹, Robert J. Gordon

Department of Chemistry, University of Illinois at Chicago (m/c 111), Chicago, IL 60607-7061, USA

Received 11 March 1994; in final form 30 August 1994

Abstract

A method is developed for extracting the photofragment speed distribution function from a velocity aligned Doppler spectrum. This method is used to determine the distribution function of HCl produced by 193 nm photodissociation of vinyl chloride. The speed distribution of the Cl fragment is determined by the method of magic angle Doppler spectroscopy.

1. Introduction

The velocity distribution of the recoiling fragments in a photodissociation reaction is useful for determining the dissociation mechanism. For example, if the internal state of one of the fragments is known, the internal energy distribution of the other fragment can be calculated from the distribution of relative kinetic energy. A useful way of obtaining this information is to measure the sub-Doppler spectrum of the state-selected fragment [1,2]. An inherent difficulty associated with Doppler spectroscopy is that it provides only the projection (w) of the velocity (v) along the line of sight. A method is required to reconstruct the speed distribution function $f(v)$ from the observed distribution of w . In the present Letter, we discuss several experimental techniques which facilitate direct inversion of the Doppler spectrum to obtain $f(v)$, and apply two of them to the UV photofragmentation of vinyl chloride.

The conventional Doppler spectrum is given by [3]

$$D(w) = \int_{|w|}^{\infty} \frac{1}{2v} [1 + \beta P_2(\cos \theta_p) P_2(w/v)] f(v) v^2 dv, \quad (1)$$

where

$$w/c = \Delta\nu/\nu_0. \quad (2)$$

Here β is the anisotropy parameter, θ_p is the angle between the polarization vector of the pump laser and the propagation direction of the probe laser, $\Delta\nu$ is the frequency shift, ν_0 is the central frequency, and c is the speed of light. If the term containing β were eliminated, $f(v)$ could be determined directly by differentiating $D(w)$ with respect to w ,

$$f(v) = -\frac{2}{v} \left. \frac{\partial D(w)}{\partial w} \right|_{|w|=v}. \quad (3)$$

A way to eliminate this term is to measure two Doppler profiles, one with the propagation vector of the probe laser parallel (D_{\parallel}) and a second with it perpendicular (D_{\perp}) to the polarization vector of the photolysis laser [4]. In the linear combination $\frac{1}{2}D_{\parallel} + D_{\perp}$ the β term drops out. A practical difficulty

¹ Permanent address: Institute for Electronic Science, Hokkaido University, Sapporo 060, Japan.

with this method is that the relative normalization of the two profiles must be known with great precision. A better technique is to measure a single profile at the magic angle $\theta_p = \cos^{-1}(3^{-1/2}) = 54.74^\circ$. This method has been used by Leone and co-workers to determine the speed distribution of $I(^2P_{1/2})$ produced from $n\text{-C}_3\text{F}_7\text{I}$ [5].

Both of these methods are limited by the requirements of a very high signal-to-noise ratio, since $f(v)$ is proportional to the derivative of the Doppler profile. This limitation is illustrated by the following numerical example. Consider the model distribution function,

$$f(v) = N \exp[-(v-v_0)^2/\sigma^2], \quad (4)$$

where v_0 is the most probable speed, σ determines the width of the distribution, and N is a normalization constant. Plots of $D(w)$ for various values of v_0/σ are shown in Fig. 1a. We see that for $v_0/\sigma < 1$ the shape of $D(w)$ is not very sensitive to v_0 , since both v_0 and σ contribute to the width of the profile. With noisy data it would be difficult to determine whether or not the distribution function peaks at zero speed.

2. Velocity aligned Doppler spectroscopy

The problems associated with conventional and magic angle Doppler spectroscopy (MADS) may be alleviated by introducing a delay t between the pump and probe lasers. This method, known as velocity aligned Doppler spectroscopy (VADS), was introduced by Wittig and co-workers [6] and further developed by Dixon et al. [7]. A requirement of this method is that the laser beams must be coaxial ($\theta_p = \pi/2$), so that after a sufficient delay only those particles moving along the line of sight are detected. As a consequence $f(v)$ can be extracted directly from a VADS profile only if β equals zero. While β is rigorously zero only if the angle between the recoil velocity vector and the transition dipole moment is 54.7° , it may otherwise have a small value if the parent molecule survives for several rotational periods before dissociating.

The VADS profile is given by

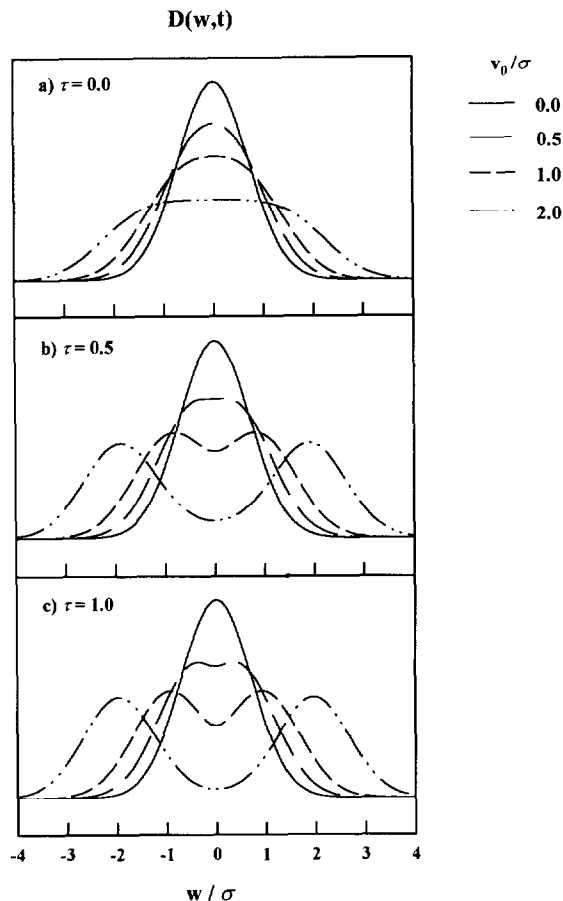


Fig. 1. Doppler profiles for the model distribution function (Eq. (4)) with different values of the reduced most probable speed v_0/σ . The curves are normalized to unit area. (a) Conventional Doppler spectrum (τ , reduced delay time) ($\tau=0$); (b) VADS with $\tau=0.5$; (c) VADS with $\tau=1.0$.

$$D(w, t) = \int_{|w|}^{\infty} \frac{1}{2v} [1 - \frac{1}{2}\beta_2 P_2(w/v)] \times F(v, w, t) f(v) v^2 dv, \quad (5)$$

where

$$F(v, w, t) = \frac{\rho^2}{\rho^2 + \alpha^2 t^2} \times \exp[-(v^2 - w^2)t^2 / (\rho^2 + \alpha^2 t^2)]. \quad (6)$$

$F(v, w, t)$ is a delay function [8] which represents the relative probability of detecting a fragment mov-

ing perpendicular to the optical axis of the laser beams after the delay time t . In Eq. (6) $\rho^2 = r_1^2 + r_2^2$, where r_1 and r_2 are the spatial Gaussian widths of the pump and probe laser profiles, assumed to be independent of the axial coordinate, and α is the most probable thermal speed of the parent molecule normal to the optical axis. Thermal motion along the line of sight will be treated later. Taking the derivative of $D(w, t)$ with respect to w and setting $|w| = v$, we obtain the result

$$f(v) = -\frac{2}{w} \frac{\rho^2 + \alpha^2 t^2}{\rho^2} \left. \frac{dD(w, t)}{dw} \right|_{|w|=v} + \frac{4t^2}{\rho^2} D(w, t) \Big|_{|w|=v}. \quad (7)$$

Eq. (7) gives the distribution function by a direct inversion of the VADS profile.

Returning to our model distribution function (Eq. (3)), we evaluated $D(w, t)$ for various reduced delay times, $\tau = \alpha t / \rho$. The Doppler profile is plotted in Figs. 1b and 1c for $\tau = 0.5$ and 1.0. Increasing τ further has little effect. We see that the VADS profile is sensitive to the value of v_0 , which is uncoupled from σ . From even a casual inspection of the VADS profile it is immediately apparent whether $f(v)$ peaks away from zero. This method is more robust than the conventional (zero delay) approach because $f(v)$ is much less sensitive to the derivative of D at large values of w .

The experimental Doppler profile $D_{\text{obs}}(w, t)$ is a convolution of $D(w, t)$ with (i) the speed distribution of the parent molecules along the line of sight and (ii) the resolution function of the probe laser; i.e.

$$D_{\text{obs}}(w, t) = D * T = \int_{-\infty}^{\infty} D(w', t) T(w - w', \alpha_{\text{eff}}) dw'. \quad (8)$$

Assuming both of these functions to be Gaussian, the transfer function $T(w, \alpha_{\text{eff}})$ is also a Gaussian with a width parameter α_{eff} ,

$$T(w, \alpha_{\text{eff}}) = \frac{1}{\alpha_{\text{eff}}(2\pi)^{1/2}} \exp(-v^2/2\alpha_{\text{eff}}^2). \quad (9)$$

The width parameter is given by [9]

$$\alpha_{\text{eff}}^2 = \frac{1}{2}\alpha^2 + \delta w^2/8 \ln 2, \quad (10)$$

where α is the most probable speed of the parent molecule, and δw is related to the bandwidth of the laser $\delta \nu$ by

$$\delta w/c = \delta \nu/v_0. \quad (11)$$

To extract $f(v)$ from the experimental profile, it is necessary first to deconvolute $D_{\text{obs}}(w, t)$. A convenient way to do this is to expand $D(w, t)$ in a set of n even harmonic oscillator functions,

$$D(w, t) = \sum_{i=0}^{n-1} a_i \phi_{2i}(w, \lambda), \quad (12)$$

where $\phi_{2i}(w, \lambda)$ is the $(2i)$ th harmonic oscillator eigenfunction with width parameter λ . Related methods have been used by Smith et al. [10], Cline et al. [11] and Aoiz et al. [12]. Expansion in an orthonormal basis has several useful properties. First, the expansion provides a global least squares fit of the data. Second, increasing the size of the basis set does not alter the values of lower coefficients. In all the data reported here, 10 basis functions converged satisfactorily. Third, using only even functions automatically symmetrizes the data with respect to positive and negative Doppler shifts. Fourth, for harmonic oscillator basis functions both forward and backwards convolution can be performed analytically [12]. Finally, the logarithmic derivative $w^{-1}d\phi_{2i}/dw$ can be determined analytically and is well behaved for all values of w .

3. Photodissociation of vinyl chloride

3.1. Experimental methods

We have used MADS and VADS to measure the speed distributions of Cl and HCl produced in the 193 nm photolysis of vinyl chloride (CH_2CHCl). The Doppler profiles were measured in a pump-and-probe apparatus described elsewhere [13]. Briefly, vinyl chloride was introduced into a vacuum chamber with a pulsed valve and dissociated with an ArF laser, while the fragments were detected by 2+1 resonance-enhanced multiphoton ionization using a frequency-doubled excimer-pumped dye laser. $\text{Cl}(^2\text{P}_{3/2})$ and $\text{Cl}(^2\text{P}_{1/2})$ were detected at the fundamental wave-

lengths 475.464 and 475.616 nm, respectively [13], while $\text{HCl}(v'=0, J'=13)$ was detected at 484.473 nm, using the P(13) line of the $\text{F}(^1\Delta, v'=0) \leftarrow \text{X}(^1\Sigma^+, v''=0)$ transition [14]. An intra-cavity étalon in the probe laser reduced the bandwidth of the fundamental to 0.04 cm^{-1} , using angle tuning for MADS and pressure tuning for VADS. In the MADS experiments the lasers were aligned at a 135° angle, with the

probe laser perpendicular to molecular beam. The polarization vector of the photolysis laser was rotated with a stack of ten quartz plates. In the VADS experiments the lasers were counter-propagated perpendicular to the direction of the molecular beam.

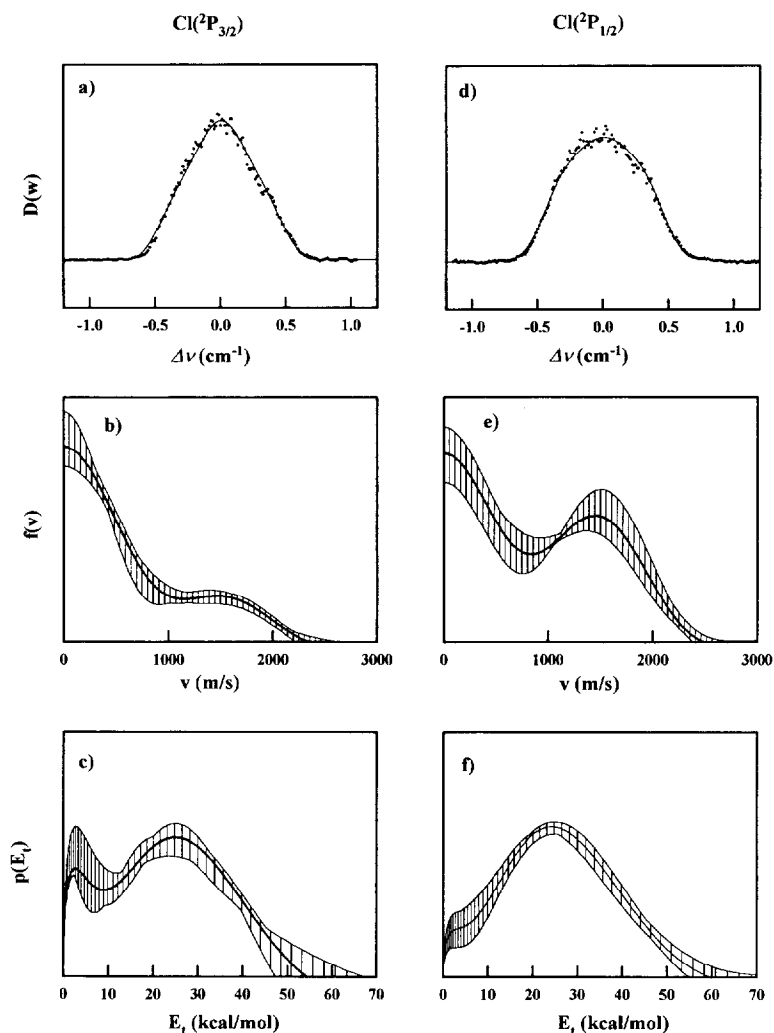


Fig. 2. MADS profiles of $\text{Cl}(^2\text{P}_{3/2})$ (panels (a)–(c)) and $\text{Cl}(^2\text{P}_{1/2})$ (panels (d)–(f)) produced in the photodissociation of vinyl chloride at 193 nm. Panels (a) and (d) are typical Doppler scans. The Doppler shift is measured with respect to the two-photon energy. The curves are least squares fits using harmonic oscillator basis functions. Panels (b) and (e) are the speed distribution functions obtained from the average of several scans using Eq. (3). Panels (c) and (f) are the kinetic energy distribution functions for the same data. The shaded regions indicate the variation between scans and the uncertainty arising from deconvolution.

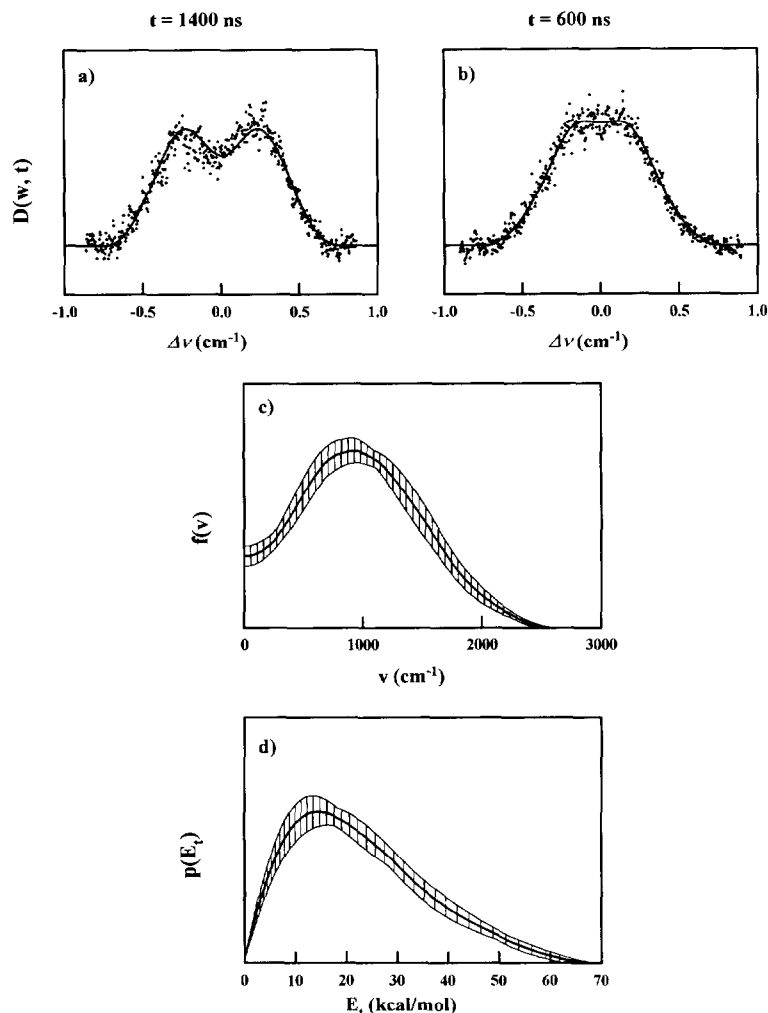


Fig. 3. VADS profiles for $\text{HCl}(v'=0, J'=13)$. Panels (a) and (b) are frequency scans obtained with delay times of 1400 and 600 ns, respectively. The Doppler shift is measured with respect to the two-photon energy. The curves are least squares fits using harmonic oscillator basis functions. Panels (c) and (d) show respectively the speed and kinetic energy distribution functions obtained with Eq. (7). The shaded areas indicate the variation arising from differences between the delay times and uncertainty in the convolution parameters.

3.2. Cl fragments

Since Mo et al. [16] found that both $\text{Cl}(^2\text{P}_{3/2})$ and $\text{Cl}(^2\text{P}_{1/2})$ recoil anisotropically, MADS is the appropriate method to use for determining the speed distributions of these fragments. The results are shown in Fig. 2. The upper panels are typical Doppler scans and harmonic oscillator fits. The middle panels show the distribution functions, $f(v)$, obtained from an average of four scans for $\text{Cl}(^2\text{P}_{3/2})$ and three for

$\text{Cl}(^2\text{P}_{1/2})$. It should be noted that the three-dimensional speed distribution function is given by $v^2f(v)$, while $f(v)$ is a one-dimensional projection. Finally, the bottom two panels show the kinetic energy distribution $p(E_i) \propto vf(v)$. The shaded regions in these panels represent the variation observed in repeated scans.

A source of systematic error in inverting D_{obs} is uncertainty in the resolution parameter, α_{eff} . Estimated bounds on α_{eff} are 0.10 to 0.18 cm^{-1} . (We estimate

that the total energy range of the two absorbed photons is two to four times the bandwidth of the laser fundamental. Additional uncertainty in α_{eff} arises from thermal motion of the parent molecule. As a worst case analysis we allowed the temperature of vinyl chloride to range from 100 to 300 K.) The uncertainty in $p(E_1)$ due to α_{eff} is included in the shaded regions of the figure.

The most striking aspect of the data is the structure observed in $f(v)$ for $\text{Cl}(^2\text{P}_{3/2})$ and $\text{Cl}(^2\text{P}_{1/2})$. Similar behavior is seen in the time-of-flight data of Umemoto et al. [17] for the total Cl signal. Mo et al. [16] showed that D_{\parallel} and D_{\perp} for both spin-orbit states could be fit by a sum of a low energy isotropic profile and a high energy anisotropic profile. A plausible interpretation of these results proposed by the previous authors is that the high energy channel results from prompt reaction on an electronically excited (e.g. n, σ^*) surface, with most of the available energy localized on the C–Cl bond, while the low energy channel results from internal conversion followed by reaction on the ground surface.

A second interesting feature of our data is the qualitatively different behavior observed for $\text{Cl}(^2\text{P}_{3/2})$ and $\text{Cl}(^2\text{P}_{1/2})$. While a double maximum is clearly evident in $p(E_1)$ for $\text{Cl}(^2\text{P}_{3/2})$, there is only a hint of a shoulder at low kinetic energy for $\text{Cl}(^2\text{P}_{1/2})$. Examination of $f(v)$, however, reveals bimodal structure for this state as well. Evidently, the extent of interaction between the two fine structure states depends strongly on the electronic state of the dissociating molecule.

We have observed similar types of behavior for the photofragmentation of the three isomers of dichloroethylene. These results will be presented in a future publication [18].

3.3. HCl fragments

In the case of HCl the signal/noise ratio was not large enough to use MADS. We found, however, that D_{\parallel} and D_{\perp} were indistinguishable, indicating that β is close to zero, allowing us to use VADS. Results of these measurements are shown in Fig. 3 for $\text{HCl}(v'=0, J'=13)$. The upper two panels are scans taken with delay times of 1400 and 600 ns. In fitting the data, the value of ρ was selected by requiring that a consistent $f(v)$ result from the two delay times.

Minimizing the sum of squares of differences between $f(v)$ derived from the two delay times gave a value of ρ between 0.9 and 1.2 mm, in good agreement with experimental estimate of 1 mm.

The striking result of this measurement is the splitting of $D(w, t=1400 \text{ ns})$, which indicates that $f(v)$ has a maximum at a speed greater than zero. This type of behavior is likely to be caused by an exit channel barrier, such as the ones predicted by Riehl and Morokuma [19]. Data for other vibrational and rotational states of HCl and a discussion of the reaction mechanism will be presented in a future publication [18].

4. Summary

Magic angle Doppler spectroscopy (MADS) was used to measure the speed distribution functions for $\text{Cl}(^2\text{P}_{3/2})$ and $\text{Cl}(^2\text{P}_{1/2})$, while velocity aligned Doppler spectroscopy (VADS) was used to measure the speed distribution function for $\text{HCl}(v'=0, J'=13)$, produced in the 193 nm photodissociation of vinyl chloride. To our knowledge this is the first time that a VADS profile has been inverted directly to obtain the speed distribution of a molecular fragment. The Cl atoms were found to have bimodal speed distributions, which is indicative of reactions occurring on two potential energy surfaces. Qualitatively different behavior was observed for the two spin-orbit states. The HCl fragment was found to have a distribution function peaked at a speed greater than zero, which is indicative of an exit channel barrier.

Acknowledgement

We have enjoyed a number of useful conversations with Dr. Andrew White, Mr. Stephan Wegerich, Professor Stephen Leone, and Professor Joseph Cline. This work was supported by the National Science Foundation (grant No. CHE-9408801) and by the Petroleum Research Fund, as administered by the American Chemical Society (grant No. 25162-AC6).

References

- [1] J. Kinsey, *J. Chem. Phys.* 66 (1977) 2560; R.N. Dixon, *J. Chem. Phys.* 85 (1986) 1866.
- [2] P.L. Houston, *J. Phys. Chem.* 91 (1987) 5388.
- [3] R. Schmiedl, H. Dugan, W. Meier and K.H. Welge, *Z. Physik A* 304 (1982) 137.
- [4] T. Sato, T. Kinugawa, T. Arikawa and M. Kawasaki, *Chem. Phys.* 165 (1992) 173.
- [5] J.I. Cline, C.A. Taatjes and S.R. Leone, *J. Chem. Phys.* 93 (1990) 6543.
- [6] Z. Xu, B. Koplitz and C. Wittig, *J. Chem. Phys.* 87 (1987) 1062; 90 (1989) 2692.
- [7] R.N. Dixon, J. Nightingale, C.M. Western and X. Yang, *Chem. Phys. Letters* 151 (1988) 328.
- [8] R.N. Dixon, J. Nightingale, C.M. Western and X. Yang, *Chem. Phys. Letters* 151 (1988) 328.
- [9] W. Demtröder, *Laser spectroscopy* (Springer, Berlin, 1981).
- [10] N. Smith, T.A. Brunner, R.D. Driver and D.E. Pritchard, *J. Chem. Phys.* 69 (1978) 1498.
- [11] C.A. Taatjes, J.I. Cline and S.R. Leone, *J. Chem. Phys.* 93 (1990) 6554.
- [12] F.J. Aoiz, M. Brouard, P.A. Enriquez and R. Sayos, *J. Chem. Soc. Faraday Trans.* 89 (1993) 1427.
- [13] P.T.A. Reilly, Y. Xie and R.J. Gordon, *Chem. Phys. Letters* 178 (1991) 511.
- [14] S. Arepalli, N. Presser, D. Robie and R.J. Gordon, *Chem. Phys. Letters* 118 (1985) 88.
- [15] R. Callaghan, S. Arepalli and R.J. Gordon, *J. Chem. Phys.* 86 (1987) 5273.
- [16] Y. Mo, K. Tonokura, Y. Matsumi, M. Kawasaki, T. Sato, T. Arikawa, P.T.A. Reilly, Y. Xie, Y. Yang, Y. Huang and R.J. Gordon, *J. Chem. Phys.* 97 (1992) 4815.
- [17] M. Umemoto, K. Seki, H. Shinohara, U. Nagashima, N. Nishi, M. Kinoshita and R. Shimada, *J. Chem. Phys.* 83 (1985) 1657.
- [18] Y. Huang, Y. Yang, G. He, S. Hashimoto and R.J. Gordon, to be submitted for publication.
- [19] J.-F. Riehl and K. Morokuma, *J. Chem. Phys.* 100 (1994) 8976.